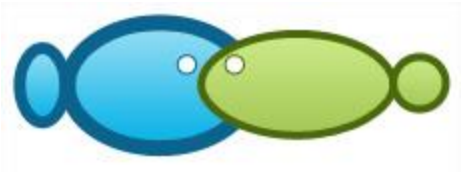

A method to quantify social relationships between captive odontocetes based on distances between individuals during synchronous breathing

[1]Kaori Tage, [2]Masatoshi Tsunokawa, [3]Hajime Ishikawa, [4]Takashi F. Matsuishi

[1] Graduate School of Fisheries Sciences, Hokkaido University, Hakodate, Hokkaido, Japan; [2] Otaru Aquarium Co. Ltd., Otaru, Hokkaido, Japan; [3] Institute of Osaka Marine Research, Taiji, Wakayama, Japan; [4] GCF, Faculty of Fisheries Sciences, Hokkaido University, Hakodate, Hokkaido, Japan. Corresponding author: T. F. Matsuishi, catm@fish.hokudai.ac.jp

Abstract. Quantifying behaviour among captive odontocetes is important for understanding the social structure and managing the captive conditions. Based on frequent interactions, trainers of captive cetaceans establish perceptions of relationships between animals. Distances between individual cetaceans during synchronous breathing can be used to express social relationships among odontocetes. If the perceptions of trainers can be visualised, these diagrams represent graphically a useful tool to improve animal care. The study aimed to both quantify social relationships among captive odontocetes, and to visualise trainer perceptions, using the distance between individuals during synchronous breathing as a metric of odontocetes social cohesion. Data were collected from three pools at three facilities housing common bottlenose dolphins or harbour porpoises. Individuals distance for dyads (a pair of cetaceans in an interactional situation) were calculated using a combination of video recordings, visual observations, and body measurements. Proximity relationships between individuals in each pool were visualised using multidimensional scaling analysis (MDS). Mathematically predicted relationships among captive odontocetes were consistent with trainer perceptions of social relationships. We demonstrated that MDS can be used to visualise social relationships among captive odontocetes, and that these visualisations can be used to assist trainers and animal management to improve captivity conditions.
Key Words: dolphin proximity, multidimensional scaling analysis, synchronous breathing.

Introduction. Dolphins may experience psychological stress in captivity due to the limited social environment (Serres et al 2020). Psychological stress can be aggravated in confined environments and limited social groups, such as captive conditions (Waples & Gales 2002). This stress can be caused by social interactions, separation of individuals, or inappropriate groupings (Waples and Gales 2002; Serres et al 2020). These stressors may result in loss of social relationships potentially leading to disease (Waples & Gales 2002). However, psychological stress in captive dolphins might be tempered if individuals have strong social bonds and can benefit from the support of conspecifics (Clegg et al 2017; Serres et al 2020). The dyads observation at a training session, keeping individuals in the same pool and segregating the individuals with negative effects for reducing the stress in the group are important for revealing the social relationships.

Social relationships among captive odontocetes should be monitored to establish and maintain minimally stressful environments (Miller et al 2021). Introducing a new animal, the death of another, or birth can change group structure and social relationships. Understanding these relationships is important for an appropriate management of the captivity (Waples & Gales 2002; Serres et al 2020). Animal caretakers often possess deep knowledge of the behaviour of individuals under their care because trainers' impressions are based on a comprehensive assessment of the daily training and observations (Whitham & Wielebnowski 2013; Khadpekar et al 2018). However, the perceptions of relationships among captive individuals and trainers are difficult to transfer to others. This is because

sensory impressions have different assessment criteria for different people and are difficult to quantify and convey to others. Depicting social relationships by means of social-structure maps has the following advantages. It can visually show social relationships, making conveying information through human communication easier. Long-term monitoring is easier because structural changes can be shown quantitatively and visually. However, to best achieve this requires the subjective impressions of trainers to be quantified.

Multidimensional scaling (MDS) is a social network analysis (Hanneman & Mark 2005). Social network analysis (SNA) can quantify the strength of relationships between individuals (Rose & Croft 2015; Davis et al 2018) and patterns within populations (Farine & Whitehead 2015; Rose & Croft 2015; Snijders et al 2017). Relationships can be defined based on interactions or associations defined by proximity (Rose & Croft 2015; Davis et al 2018). SNA can depict social relationships among individuals within a group, illustrating individual social connections, and the strength of preferential relationships with others (Rose & Croft 2015). MDS can quantify and visualise similarities within a group using a proximity matrix representing the distance between pairs of cetaceans (dyads) in interactional situations, the result of which depicts spatial relationships among individuals (Hout et al 2013).

MDS using individual distance (ID) was applied to captive Iberian wolves *Canis lupus signatus* and successfully represented pack cohesion (Soriano et al 2020). ID represents the minimum distance an animal routinely maintains between itself and other members of the same species (Hediger 1950). It has been used to identify social relationships in various animal groups, and can be influenced by relationships between members within a group (Kummer 1970; Warburton & Lazarus 1991) and familiarity, social rank, sex and age (Shuji 1995; Sakai et al 2010; Soriano et al 2020). Quantifying ID might assist with the identification of social relationships among captive odontocetes. Synchronous breathing occurs when two or more dolphins simultaneously breathe on the surface (Connor et al 2006), which is considered as having a functional role in maintaining relationships within swimming dyads, because it can be influenced by pod social structure, kinship level, age, and sex (Sakai et al 2010; Actis et al 2018; Serres et al 2021), therefore it can be used as an index of cohesion and sociality among individuals (Actis et al 2018). This index could be a useful and easily measured tool to assess cetacean sociality when individuals can be identified above water (Sakai et al 2010; Senigaglia & Whitehead 2012; Actis et al 2018). Synchronous breathing of pairs might also be easy to observe from the water in aquaria because the numbers of individuals in pools are low enough to enable accurate identification. In the case of this study, the objective is to depict the trainers' perceptions by using MDS, so it is necessary to measure a meaningful ID. In addition, in order to calculate accurate IDs, it is necessary to select a moment when the IDs are not distorted when viewed from above the water surface. Odontocete ID during synchronous breathing has been well-studied (Connor et al 2006; Sakai et al 2010; Senigaglia & Whitehead 2012; Actis et al 2018; Serres et al 2021). For wild Indo-Pacific bottlenose dolphins, *Tursiops aduncus*, at Mikura Island, Japan, ID during synchronous breathing was shortest between female and calf pairs, and shorter in female pairs than in male pairs, and relationships changed depending on the sex or age of the pairs (Sakai et al 2010). Indo-Pacific bottlenose dolphins may have strong mother-offspring bonds and associate with other females to help rear calves (Wang 2018). Social relationships among captive odontocetes could be expressed in aquaria using ID during synchronous breathing. It is difficult to apply the methods of previous research to the captivity condition, so these methods are needed to be improved for use in aquaria.

Firstly, surface video could be used to record and observe synchronous breathing. For wild odontocetes, this breathing has been observed using video taken from helicopters, boats, or on SCUBA (Connor et al 2006; Sakai et al 2010; Senigaglia & Whitehead 2012; Actis et al 2018; Smultea et al 2018). Because the synchronous breathing rate of captive odontocetes increases under stress, for example, when a diver is in a pool (Serres et al 2021), it would be inappropriate to observe surface breathing behaviour in captivity. Surface video is not easy in aquarium environments using a drone to obtain the video. Therefore, it is necessary to track odontocetes above water and fix the cameras looking down over a pool from above in the case of aquaria. Secondly, ID has been estimated from

distances between animals' body (Connor et al 2006; Sakai et al 2010; Senigaglia et al 2012; Senigaglia & Whitehead 2012; Serres et al 2021). The image is distorted because the video is typically recorded from seats, in an oblique position.

Moreover, an animal's size in images varies depending on where it was situated in an aquarium, relatively to the camera, which involved coefficients of correction. Hence, IDs determined from animals in images might differ from actual IDs. The study aimed to develop a method based on video recordings above the surface to quantify and visualise social relationships among captive odontocetes consistently with trainers' perceptions. MDS was applied for visualising trainers' perceptions. The ID of dyads at synchronous breathing was calculated from surface video to obtain the proximity matrices for MDS. This method was applied to three pools at two aquariums for experimental purposes and demonstrated the examples that could be obtained. This experiment does not intend to examine captive odontocetes' social structures in the pools.

Material and Method

Quantifying social relationships

Coordinate correction. To convert video image locations to actual locations on the surface of pools, formulas to correct coordinates are presented. Video cameras were installed as far as possible from the pools to record the entire pool surface (Figure 1).

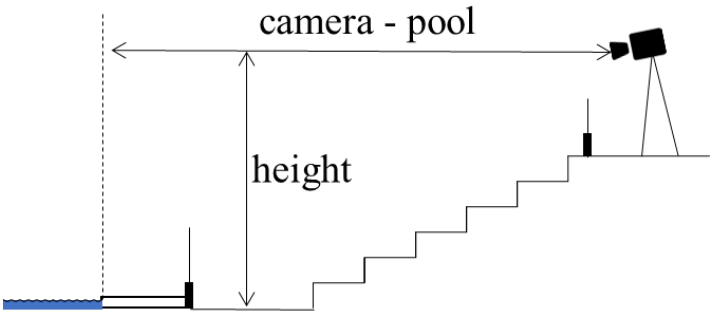

Figure 1. Pool and camera positions.

The video was recorded while a levelling rod marked every 20 cm (TAJIMA, HRD-100, 1 m) with plastic strings attached to either end, or a disc (30 cm diameter, 5 mm thick, white acrylic) with two holes and plastic strings, was moved over the surface of the pool from the back to front (Y-axis) and left to right (X-axis), towards the video camera. Since the correction formula is obtained in each facility, it does not matter if the size of the scale differs from facility to facility as long as the scale is large enough to be visible on the image. These scales were moved the appropriate number of times to ensure that no excess or deficiency depended on the pool size. The levelling rod was only used in the Otaru aquarium, but the disc was used in the Dolphin Resort. The disc proved easier to record than the levelling rod. Because disc diameter remained constant in all directions, the X and Y axes could be recorded simultaneously when the disc moved over the entire pool. Stills were captured from video using Adobe Premiere Pro v 14.7.0 (build 23). Images were chosen when the scale (levelling rod or disc) was not distorted on the water surface. XY pixel coordinates on the scale were acquired every 20 (levelling rod) or 30 cm (disc) from captured images using ImageJ v 1.53e. Here, XY pixel coordinates on the captured images were recorded. Midpoints of XY pixel coordinates every 20 or 30 cm on the scale were calculated. The 20 or 30 cm in length was divided by the distance between acquired XY pixel coordinates (z) to calculate how many centimetres one pixel represented (cm pixel^{-1}). Values of z are defined as representative values for each midpoint. The multiple regression conversion equations of the X and Y axes (Z_x and Z_y) were derived using values for the midpoint and z. The derivation of Z_x and Z_y and the calculation of multiple correlation coefficients were performed using the regression analysis function in Microsoft Excel. Values of $z$were plotted on the contour maps for both X and Y axes toward the video camera using the "akima" package (Akima 2020) in R studio 1.4.1103. Z_x and Z_y with larger

multiple regression coefficients were modified by removing the outliers of *z* referring to the contour maps since it was difficult to find values that did not fit on the contour lines until all *z* values were plotted. Locations of odontocetes were converted from surface images using Z_x and Z_y. Z_x and Z_y were represented as $AX_p + BY_p + C$ and $A'X_p + B'Y_p + C'$, respectively, at the pixel coordinate (X_p, Y_p) on images, so the coordinate (X, Y) on the surface of the pool was represented by $\left(\sum_{k=1}^{X_p} Z_x, \sum_{k=1}^{Y_p} Z_y\right)$. Therefore, the coordinate (X, Y) was calculated by the formulas:

$$X = \frac{A}{2} X_p\left(X_p + 1\right) + X_p\left(BY_p + C\right)$$

$$Y = \frac{B'}{2} Y_p\left(Y_p + 1\right) + Y_p\left(A'X_p + C'\right)$$

ID calculation. The odontocete shape was simplified into a pentagon (Figure 2), with the shortest distance between two odontocetes calculated as the distance between the pentagon vertices. The pentagon was assumed to be bilaterally symmetrical with respect to the beak-fluke axis on the horizontal plane.

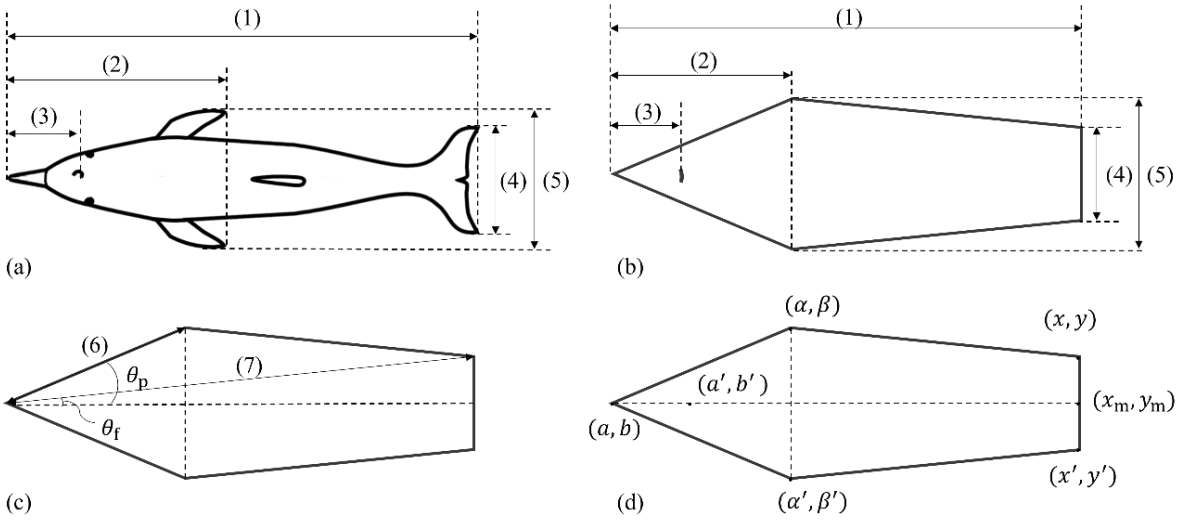

Figure 2. (a)(b) Body Measurement (c) calculations to determine dolphin or porpoise body shape (d) Coordinates to acquire vertices of a pentagon.
(a) and (b) (1) Body length (from the tip of the rostrum to the tip of the fluke), (2) rostrum–flipper width (from the tip of the rostrum to the midpoint of the maximum width of left and right flippers), (3) rostrum–blowhole length (from the tip of the rostrum to the middle of the blowhole), (4) flipper–flipper width (the maximum width between left and right flippers), and (5) fluke width (the maximum width of the fluke). (c) values to calculate vertices of a pentagon: (6) length of the rostrum–right flipper segment (from the tip of the rostrum to the right point of the maximum width of left and right flippers), (7) length of the segment from the rostrum to the right fluke (the distance between the tip of the rostrum and the midpoint of the maximum width of fluke); θ_p is the angle formed by the body length axis (1) and the rostrum–right flipper axis (6); θ_f is the angle formed by (1) body length axis and (7) the rostrum–right fluke axis. (d) (a, b) is the coordinate of the tip of the rostrum; (a', b') is the coordinate of the middle of the blowhole; (α, β) is the coordinate of the right point of the left and right flipper axis; and (α', β') is the coordinate of the left point of the left and right flipper axis.

Measurement of odontocetes and calculation of vertices of the pentagons. Body measurements of each animal were made to calculate vertices for individual pentagons for each individual in each pool. Measurements include lengths of (1) body, (2) rostrum–flipper segment, (3) rostrum–blowhole segment, (4) fluke, and (5) flipper–flipper segment (Figure

2, (a) and (b)). Using measurements (1)–(5), $\cos\theta_p$, $\sin\theta_p$, $\cos\theta_f$, $\sin\theta_f$, the length of the rostrum–right flipper segment (6) and the length of the rostrum–right fluke segment (7) of Figure 2 (c) were calculated using the equation in Table 1. Pentagon vertices (Figure2 (d)) are calculated by the rotation matrix using values for (1), (3), (8), (9), $\cos\theta_p$, $\sin\theta_p$, $\cos\theta_f$, and $\sin\theta_f$ for each odontocete using equations in Table 1 (All trigonometric functions, notations and coordinates correspond to values in Figure 2), after calculating the coordinates of the rostrum and middle of the blowhole from captured images using ImageJ.

Table 1

Body measurements and calculations used to acquire pentagon vertices

Measurement/ Calculation items	*Corresponding notation in figures*	*Measured or obtained value/calculation*
Body length	(1)	Measured value
Rostrum-flipper	(2)	Measured value
Rostrum-blowhole	(3)	Measured value
Fluke	(4)	Measured value
Flipper-flipper	(5)	Measured value
Rostrum-right point of flipper	(6)	$\sqrt{((2))^2+\left(\frac{(5)}{2}\right)^2}$
Rostrum-right point of fluke	(7)	$\sqrt{((1))^2+\left(\frac{(4)}{2}\right)^2}$
The ratio of the rostrum to the right point of the flipper segment against the body length	(8)	$\frac{(6)}{(1)}$
The ratio of the rostrum to the right point of the fluke segment against the body length	(9)	$\frac{(7)}{(1)}$
$\cos\theta_{\mathrm{p}}$	$\cos\theta_{\mathrm{p}}$	$\frac{(2)}{(6)}$
$\sin\theta_{\mathrm{p}}$	$\sin\theta_{\mathrm{p}}$	$\frac{(5)/2}{(6)}$
$\cos\theta_{\mathrm{f}}$	$\cos\theta_{\mathrm{f}}$	$\frac{(1)}{(7)}$
$\sin\theta_{\mathrm{f}}$	$\sin\theta_{\mathrm{f}}$	$\frac{(4)/2}{(7)}$
Coordinate of rostrum	(a,b)	Obtained value from the images
Coordinate of blowhole	(a',b')	Obtained value from the images
Coordinate of the right point of the maximum width of left and right flippers	(α,β)	$\begin{pmatrix}\{(x_{\mathrm{m}}-a)\cos\theta_{\mathrm{p}}-(y_{\mathrm{m}}-b)\sin\theta_{\mathrm{p}}\}\times(8)+a,\\ \{(x_{\mathrm{m}}-a)\sin\theta_{\mathrm{p}}+(y_{\mathrm{m}}-b)\cos\theta_{\mathrm{p}}\}\times(8)+b\end{pmatrix}$
Coordinate of the left point of the maximum width of left and right flippers	(α',β')	$\begin{pmatrix}\{(x_{\mathrm{m}}-a)\cos\theta_{\mathrm{p}}-(y_{\mathrm{m}}-b)(-\sin\theta_{\mathrm{p}})\}\times(8)+a,\\ \{(x_{\mathrm{m}}-a)(-\sin\theta_{\mathrm{p}})+(y_{\mathrm{m}}-b)\cos\theta_{\mathrm{p}}\}\times(8)+b\end{pmatrix}$
Coordinate of the right point of the maximum width of the fluke	(x,y)	$\begin{pmatrix}\{(x_{\mathrm{m}}-a)\cos\theta_{\mathrm{f}}-(y_{\mathrm{m}}-b)\sin\theta_{\mathrm{f}}\}\times(9)+a,\\ \{(x_{\mathrm{m}}-a)\sin\theta_{\mathrm{f}}+(y_{\mathrm{m}}-b)\cos\theta_{\mathrm{f}}\}\times(9)+b\end{pmatrix}$
Coordinate of the left point of the maximum width of the fluke	(x',y')	$\begin{pmatrix}\{(x_{\mathrm{m}}-a)\cos\theta_{\mathrm{f}}-(y_{\mathrm{m}}-b)(-\sin\theta_{\mathrm{f}})\}\times(9)+a,\\ \{(x_m-a)(-\sin\theta_{\mathrm{f}})+(y_{\mathrm{m}}-b)\cos\theta_{\mathrm{f}}\}\times(9)+b\end{pmatrix}$
Coordinate of the midpoint of the maximum width of the fluke	$(x_{\mathrm{m}},y_{\mathrm{m}})$	$\left(\frac{(1)\times a'-a\times((1)-(3))}{(3)},\frac{(1)\times b'-b\times((1)-(3))}{(3)}\right)$

Distance calculation. Since the rostrum and blowhole during synchronous breathing was captured, it was assumed that the odontocetes were approximately on the same plane, assuming the wave on the water surface is negligible.

1. The vertices of each pentagon are defined as the convex points on the body of odontocetes: the rostrum, both ends of the maximum width of the left and right flippers, and both ends of the maximum width of the fluke (Figure 2(d)).
2. The shortest distance between two individuals is represented by the minimum distance between the combinations of vertices in two pentagons because the odontocete shape was simplified into a pentagon. There are 25 possible distances between two individuals with 5 vertex combinations, of which only one is the shortest.
3. Cross product was calculated using each edge vector of one individual and the convex points of the other individual, to discriminate if two animals were superimposed. The positive or negative signs of the cross products of one vertex of the arbitrary pentagon and each of the five sides of another pentagon are all matched when pentagons were superimposed. Distance is defined as zero cm when two pentagons partly overlap in cross-product calculation results.
4. Thus, all ID values (d_{ij}) represent either the shortest distance between vertices of two pentagons or zero cm (overlap).

Calculation of indices of mean ID for MDS. An index of the mean distance was defined for each dyad, d_i, by calculating the mean ID during the synchronous breathing frequency (f_i) found in whole observation period. Social relationships among odontocetes in each pool are described by MDS using the distance matrices of d_i, where f_i represents the number of images available for ID calculation. Each ID for each dyad is represented as d_{ij}, where j represents each synchronous breath. d_i is represented as:

$$d_i = \frac{1}{f_i}\sum_{j=1}^{f_i} d_{ij}$$

Describing social relationships by MDS. The distance matrix for all dyads was created by d_i. Social relationships among captive odontocetes in each pool were described using MDS from this distance matrix. MDS results were prepared using the "igraph" package (Csardi et al 2006) in R studio 1.4.1103. When the distance between dyads on the surface at the synchronous breathing is shorter, the individuals are plotted closer in two-dimensional space on MDS than those with a long distance on the surface. By assessing the distance between dyads on a map, one obtains a quantitative measurement of perceived similarities relatively to other individuals in two-dimensional space (Hanneman & Mark 2005; Hout et al 2013). MDS outcomes were investigated to determine if they were consistent with trainer perceptions. When illustrated in MDS, lines between individuals represent relative IDs.

Interviews. Before analysing MDS, we interviewed trainers about the perceptions of social relationships between odontocetes under their care. The results of interviews were used to determine if the outcome of MDS with d_i matched their impressions. The trainer's daily observations on the social relationships among captive odontocetes were investigated.

Applications. We tested whether this method, which expresses individual relationships by MDS, is consistent with the trainer's perceptions. Data were collected for three pools at three facilities (Table 2): the Dolphin Stadium and a Display pool in the Otaru Aquarium (Otaru, Hokkaido, Japan), and an 11.0 m diameter pool at the Dolphin Resort (Taiji, Wakayama Prefecture Japan). Video cameras were placed where the entire surface pool could be seen. The focus was fixed on the middle of the pool.

Table 2

Camera installation locations, visual observations and recordings by facility

Pool	*Height (m)*	*Camera–pool (m)*	*Observable pool size (m) L×W or diameter*	*Observation time (min)*	*Study period (yyyy.mm.dd hh:mm)*
Otaru Aquarium Display pool	3.8	2.4	12.0	943	2019.11.28 09:00-16:00 2019.11.29 08:30-16:00 2019.11.30 08:30-15:40
Otaru Aquarium Dolphin Stadium	4.5	12.5	78.0×33.0	948	2020.11.28 08:50-16:00 2020.11.29 08:30-16:00 2020.11.30 08:30-16:00
Dolphin Resort 11.0 m circular pool	7.7	11.0	11.0	1079	2021.07.13 11:50-16:00 2021.07.14 09:20-17:00 2021.07.15 09:10-17:00

Visual observations and video recordings. Visual observations and video recordings were made in all pools outside training and dolphin showtimes. Video cameras were placed where the entire pool could be seen. The focus was fixed on the middle of the pool. Cameras were always at the same position throughout the data collection after installation. Different cameras were used for different pools. At the Otaru Aquarium Dolphin Stadium and Dolphin. Resort circular pool, odontocete behaviour and video of scales were filmed using a camcorder (SONY FDR-AX 700) with a recording format 2160/30p 60 Mbps (XAVC S 4K) and a circular polarising light filter (SONY VF-62CPAM2) mounted on a camera tripod (Velbon Medium Aluminium Tripod EX-547). A web video camera (Logitech HD Pro Webcam C920 with USB2.0 and 12 m of extension cable KB-USB-R212), camera tripod (SLIK Compact II), and recording software (Logitech Capture 1.10.110, 24 fps, 640 × 360 resolution) were used at the Otaru Aquarium Display pool. The time, pairs involved in synchronous breathing, and any notable events were recorded by an observer positioned as far as possible from the dolphins because individual identification and determining any lag in synchronous breathing were difficult to achieve from video imagery (Figure 3.). Video images were used for ID calculation and to identify behaviour before synchronous breathing, and visual observations were used to determine the individuals involved and f_i, the synchronous breathing frequency.

Synchronous breathing. We recognise three patterns (1–3) in synchronous breathing based on whether two odontocetes: 1) swam parallel to each other and simultaneously broke the surface; 2) did not swim parallel to each other but broke the surface simultaneously in the same direction; or 3) first breathed separately despite swimming parallel to each other, and then swam parallel to each other and broke the surface simultaneously. In this study, cases in which individuals breathed synchronously but had not swum parallel in the same direction, or where one individual had jumped during synchronous breathing were excluded because breathing without the same movement falls outside the definition of synchronous breathing.

(a) (b) (c)

Figure 3. Images captured from the video (a) the Otaru aquarium Display pool, (b) the Otaru aquarium Dolphin Stadium, (c) Dolphin Resort circular pool.

The Otaru Aquarium Display pool. Two female (A, M) and two male (S, T) harbour porpoises (*Phocoena phocoena*) at the Otaru Aquarium Display pool (12.0 m diameter) were observed from 11–13 December 2019. Table 3 shows measurements of harbour

porpoises in the pool. The video camera was installed at 3.8 m height and 2.4 m away from the pool (Table 2). The levelling rod was moved on the water surface seven times back to front and six times left to right towards the web video camera. The results of multiple regression conversion formulas for converting video image locations to actual locations on the surface of pools are:

$$Z_x = 0.0019X_p + 0.014Y_p - 0.30 \ (R^2 = 0.88),$$
$$Z_y = 0.0080Y_p + 0.0035X_p - 14 \ (R^2 = 0.81).$$

The total observation time was 943 min (Table 2). Visual observations and video recordings identified patterns of synchronous breathing 1 and 2 for each dyad. Observed mean ID and frequency of synchronous breathing are listed by dyads in Table 4. The total f_i for all six dyads was 713. The shortest d_i was calculated for dyad AT, and the longest for dyad AM. The highest f_i was observed for dyad AT, and the lowest for dyads AS and ST.

Table 3

Measurements of Harbour porpoises in the Otaru Aquarium Display pool

Porpoise code	*Sex*	*Measurements (cm)*				
		(1)	*(2)*	*(3)*	*(4)*	*(5)*
A	F	185	45	15	43	52
M	F	173	60	14	38	42
S	M	158	50	18	39	43
T	M	161	46	20	39	45

(1)–(5) correspond to notations in Figures 2. and Table 1. Porpoises were measured on 26 December 2019.

Table 4

Dyad d_i and f_i values for the Otaru Aquarium Display pool

Dyad	*d_i (cm)*	*f_i*
AM	148	100
AS	129	22
AT	69	249
MS	145	126
MT	128	194
ST	133	22

f_i is the frequency of synchronous breathing; d_i is our index of mean ID for each dyad.

The Otaru Aquarium Dolphin Stadium. Three male (A, N, R) common bottlenose dolphins (*Tursiops truncatus*) were housed in the Dolphin Stadium of the Otaru Aquarium (Table 5) within a rectangular pool 78.0 × 33.0 m. Observations were conducted from 28–30 November 2020. The camcorder was installed at 4.5 m in height and 12.5 m away from the pool (Table 2). A levelling rod was moved over the water surface seven times back to front and four times left to right towards the camcorder. The results of multiple regression conversion formulas are:

$$Z_x = -0.000011X_p + 0.00057Y_p + 0.041 \ (R^2 = 0.61)$$
$$Z_y = 0.0021Y_p - 0.000098X_p - 0.35 \ (R^2 = 0.30)$$

Table 5

Measurements of male bottlenose dolphins in the Otaru Aquarium Dolphin Stadium

Dolphin code	*Measurements (cm)*				
	(1)	*(2)*	*(3)*	*(4)*	*(5)*
A	266	56	35	58	84
N	303	73	38	65	94
R	316	76	42	68	97

(1)–(5) correspond to notations in Figures 2 and Table 1. Dolphins were measured on 29 November 2020.

The total observation time was 498 min (Table 2). Visual observations and video recordings identified patterns 1–3 of synchronous breathing for each dyad. Measurements of male bottlenose dolphins in the Otaru Aquarium Dolphin Stadium were shown in Table 5. The total f_i for all three dyads was 148. The shortest d_i was calculated for dyad NR, the longest for dyad AN. Observed mean ID and frequency of synchronous breathing for the Otaru Aquarium Dolphin Stadium are listed by dyads in Table 6. The highest f_i was observed for dyad NR, which was the lowest f_i for dyad AN.

Table 5

Dyad d_i and f_i values for the Otaru Aquarium Dolphin Stadium

Dyad	*d_i (cm)*	*f_i*
AN	312	15
AR	288	53
NR	230	80

f_i is the frequency of synchronous breathing; d_i is our index of mean ID for each dyad.

Dolphin Resort circular pool. Four male (C, F, G, H) common bottlenose dolphins in this pool were observed from 13–16 July 2021. Measurements of the dolphins were shown in Table 7. The camcorder was installed on the roof of an adjacent building at 7.7 m in height and 11.0 m away from the pool (Table 2).

The disc was moved on the water surface eight times back to front and seven times left to right towards the camcorder. The results of multiple regression conversion formulas are:

$$Z_x = -0.00000081X_p + 0.00010Y_p + 0.18 \ (R^2 = 0.96),$$
$$Z_y = 0.00041Y_p + 0.000039X_p + 0.17 \ (R^2 = 0.61).$$

The total observation time was 1079 min (Table 2). Visual observations and video recordings identified patterns 1–3 of synchronous breathing for each dyad. Observed mean ID and frequency of synchronous breathing are listed by dyads in Table 8. The total f_i for all six dyads was 454. The shortest d_i was calculated for dyad CF, and the longest was calculated for the dyad CG. The highest f_i was observed for dyad CF, and the lowest was observed for the dyad FG (Table 8).

Table 6

Measurements of male bottlenose dolphins in the Dolphin Resort 11.0 m diameter pool

Dolphin code	*Measurements (cm)*				
	(1)	*(2)*	*(3)*	*(4)*	*(5)*
C	297	97	42	66	79
F	296	89	38	65	76
G	302	95	40	68	78
H	307	97	42	71	74

(1)–(5) correspond to notations in Figures 2 and Table 1. Dolphins were measured on 19 July 2021.

Table 7

Dyad d_i and f_i values for the Dolphin Resort 11.0 m diameter pool

Dyad	*d_i (cm)*	*f_i*
CF	23	305
CG	73	6
CH	60	14
FG	49	4
FH	42	25
GH	32	100

f_i is the frequency of synchronous breathing; d_i is our index of mean ID for each dyad.

Results. MDS in each pool were described using the distance matrix of d_i.

Application in the Otaru Aquarium Display pool. The AT dyad had a high f_i and shortest d_i (d_{AT}=69 cm, f_{AT}=249 in 943min). M seldom coordinated synchronous breathing with other individuals (f_{AM}=100, f_{MS}=126, f_{MT}=194). The f_i of S and other individuals was low (f_{AS}=129, f_{MS}=126, f_{ST}=22). Assuming that physical distance reflects social distance, the affiliative dyads were considered to have the shorter ID. Therefore, as revealed in the MDS outcome (Figure 4.), the result of the relative distance relationships using d_i (our index of mean ID for each dyad), A and T are relatively close, and M and S are relatively distant.

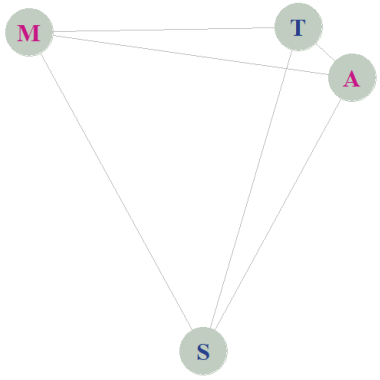

Figure 4. Outcome of MDS with d_i for the Otaru Aquarium Display pool.

Application in the Otaru Aquarium Dolphin Stadium. The NR dyad had a high f_i and the shortest d_i (d_{NR}=230cm f_{NR}=80 in 948 min). A had a seldom coordinated synchronous breathing with other individuals (f_{AN}=15, f_{AR}=53). A did synchronous breathing far from others (d_{AN}=312, d_{AR}=288). In the interview, the trainer recognised that N and R had an affiliative relationship, but A and N did not. According to the trainer's daily observations, A and N often engaged in aggressive behaviours such as chasing or biting, while N and R swam together. However, trainers also said, "A and N did not engage in aggressive behaviours and kept their distance when the two were put together. Therefore, the relationships of the three animals were not completely without affinity only when all three were put together. It would be difficult to house or train the dolphins in the same pool if the three animals were not entirely compatible". The MDS outcome (Figure 5.), show that A was distanced from R and N, which is consistent with the trainer's perceptions.

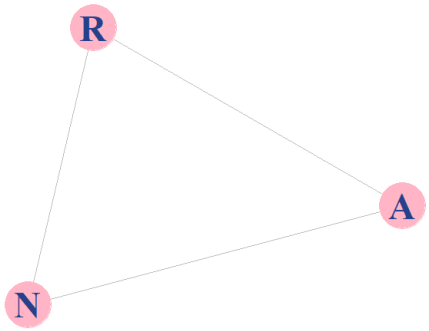

Figure 5. Outcome of MDS with $\boldsymbol{d_i}$ in the Otaru Aquarium Dolphin Stadium pool.

Application in the Dolphin Resort circular pool. The CF dyad had a high f_i and the shortest d_i (d_{NR}=23 cm, f_{NR}=305 in 1079 min). H had a seldom coordinated synchronous breathing with other individuals (f_{CH}=14, f_{FH}=25), except for G (f_{GH}=100). The trainer perceived "H to be the dominant specimen among the four dolphins, and C and F often swim together". According to the trainer's daily observations, H had the least number of tooth rake marks of the four animals and often bit other dolphins. The d_i (our index of mean ID for each dyad) was calculated from d_{ij} (all IDs for each dyad) and f_i (synchronous

breathing frequency). The trainer also indicated that "it was once possible to perform husbandry training with both G and H simultaneously, but with the increased social ranking of H this was now impossible; H had to be alone". The outcome of MDS (Figure 6), in which H was placed farther from other individuals, was consistent with trainer perceptions.

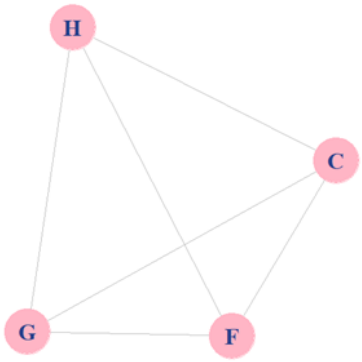

Figure 6. Outcome of MDS with d_i in the Dolphin Resort circular pool.

Discussion. These results suggest that MDS using d_i successfully expresses social relationships among captive odontocetes. The outcomes illustrated by MDS are consistent with trainer perceptions based on visual observations of dolphin and porpoise behaviours in pools. In this study, MDS was described using d_i (our index of mean ID for each dyad) calculated from (our index of mean ID for each dyad) calculated from d_{ij} (all IDs for each dyad) and f_i (synchronous breathing frequency). Affiliative dyads typically have a shorter d_i and a higher f_i, like AT in the Otaru Aquarium Display pool. This indicates that the shorter the ID during synchronous breathing, the higher the synchronous breathing frequency in captive conditions, as in the wild (Connor et al 2006; Actis et al 2018). Social relationships illustrated by MDS are consistent with trainer perceptions based on visual observations of dolphin and porpoise behaviours in pools. These results suggest that MDS using d_i successfully expresses social relationships among captive odontocetes, even where trainers have not discerned social relationships because of new introductions, the death of individuals in a population, population reconstruction or a population that is new to a trainer. In addition to verbal communication, MDS plots can assist trainers in determining the proper dyads for the training, social order, and the change of social relationships with the growth and maturation because quantified social relationships can be used to evaluate the social structure or stability. The ID during synchronous breathing in wild odontocetes is affected by kinship and sex (Sakai et al 2010; Serres et al 2021). Continued observations might reveal the effects of calf development, new introductions and class changes on social relationships. Captive dolphins can experience stress stemming from social interactions (Waples & Gales 2002; Clegg et al 2017; Serres et al 2020). Because social relationships reported herein are manifest for a narrow window of time, prolonged and recurring observations should be made, such as when a new individual is introduced into an aquarium environment or after an individual's death. The method was applied for three to five captive odontocetes in this study. The most accurate ID could be calculated using the fixed camera and multiple regression conversion equations. The observation was conducted for three days, but MDS could visualise trainers' perceptions even during a short-term observation. Therefore, this method can apply to the larger group and provide snapshots of the dolphins if only the individuals can be identified.

Conclusions. The study showed that MDS can describe social relationships among captive odontocetes with d_i as an index of individual distance, and was consistent with trainer perceptions of relationships between captive animals. MDS enables the quantification of social relationships among captive odontocetes and visualises trainer perceptions. Ongoing analysis will enable changes in relationships between captive cetaceans to be identified early, and adjustments made to improve long-term animal welfare.

Acknowledgements. The authors are grateful to the Otaru Aquarium and Dolphin Resort trainer teams, who permitted this study in their facilities. We also thank Ms Suzuki H., the Future University of Hakodate, for her kind assistance in the experiment. Dr Steve O'Shea from Edanz (https://jp.edanz.com/ac) edited a draft of this manuscript. This research did not receive any specific grant from funding agencies in the public, commercial, or non-profit sectors.

Conflict of interest. The authors declare no conflict of interest.

References

Actis P. S., Danilewicz D., Cremer M. J., Bortolotto G. A., 2018 Breathing synchrony in franciscana (*Pontoporia blainvillei*) and Guiana dolphins (*Sotalia guianensis*) in Southern Brazil. Marine Mammal Science 34:777–789.

Akima H., Gebhardt A., 2020 Interpolation of Irregularly and regularly spaced data. R package version 0.6-2.1. https://CRAN.R-project.org/package=akima

Clegg I. L. K., Rödel H. G., Delfour F., 2017 Bottlenose dolphins engaging in more social affiliative behaviour judge ambiguous cues more optimistically. Behavioural Brain Research 322:115–122.

Connor R. C., Smolker R., Bejder L., 2006 Synchrony, social behaviour and alliance affiliation in Indian Ocean bottlenose dolphins, *Tursiops aduncus*. Animal Behaviour 72:1371–1378.

Csardi G., Nepusz T., 2006 The igraph software package for complex network research. InterJournal, complex systems, 1695.

Davis G. H., Crofoot M. C., Farine D. R., 2018 Estimating the robustness and uncertainty of animal social networks using different observational methods. Animal Behaviour 141:29–44.

Farine D. R., Whitehead H., 2015 Constructing, conducting and interpreting animal social network analysis. Journal of Animal Ecology 84:1144–1163.

Hanneman R. A., Riddle M., 2005 Introduction to social network methods. University of California, Riverside, http://faculty.ucr.edu/~hanneman/.

Hediger H., 1950 Wild animals in captivity. Butterworths Scientific Publications, London, 218 p.

Hout M. C., Papesh M. H., Goldinger S. D., 2013 Multidimensional scaling. Wiley Interdisciplinary Reviews: Cognitive Science 4:93–103.

Khadpekar Y., Whiteman J. P., Durrant B. S., Owen M. A., Prakash S., 2018 Approaches to studying behavior in captive sloth bears through animal keeper feedback. Zoo Biology 37:408-415.

Kummer H., 1970 Spacing mechanisms in social behavior. Social Science Information 9:109–122.

Miller L. J., Lauderdale L. K., Mellen J. D., Walsh M. T., Granger D. A., 2021 Assessment of animal management and habitat characteristics associated with social behavior in bottlenose dolphins across zoological facilities. PLoS One 16:e0253732.

Rose P. E., Croft D. P., 2015 The potential of social network analysis as a tool for the management of zoo animals. Animal Welfare 24:123-138.

Sakai M., Morisaka T., Kogi K., Hishii T., Kohshima S., 2010 Fine-scale analysis of synchronous breathing in wild Indo-Pacific bottlenose dolphins (*Tursiops aduncus*). Behavioural Process 83:48–53.

Senigaglia V., de Stephanis R., Verborgh P., Lusseau D., 2012 The role of synchronised swimming as affiliative and anti-predatory behavior in long-finned pilot whales. Behavioural Process 91:8–14.

Senigaglia V., Whitehead H., 2012 Synchronous breathing by pilot whales. Marine Mammal Science 28:213–219.

Serres A., Hao Y., Wang D., 2020 Body contacts and social interactions in captive odontocetes are influenced by the context: An implication for welfare assessment. Animals 10:924.

Serres A., Hao Y., Wang D., 2021 Contextual impacts on individual and synchronous breathing rate variations in three captive odontocete groups. Zoo Biology 40:20–32.
Shuji Y., 1995 Affinity within the herd. Japanese Journal of Livestock Management 31:44–50.
Smultea M. A., Lomac-MacNair K., Nations C. S., McDonald T., Würsig B., 2018 Behavior of Risso's dolphins (*Grampus griseus*) in the Southern California bight: An aerial perspective. Aquatic Mammals 44:653–667.
Snijders L., Blumstein D. T., Stanley C. R., Franks D. W., 2017 Animal social network theory can help wildlife conservation. Trends in Ecology & Evolution 32:567-577.
Soriano A. I., Vinyoles D., Maté C., 2020 Inter-individual distance in different captive packs of Iberian Wolf (*Canis lupus signatus*): Management applications. Journal of Applied Animal Welfare Science 24:72-82.
Wang J. Y., 2018 Bottlenose dolphin, *Tursiops aduncus*, Indo-Pacific bottlenose dolphin. In: Encyclopedia of marine mammals. Würsig B., Perrin W. F., Thewissen J. G. M. (eds), pp 125–130, Academic Press, London.
Waples K. A., Gales N. J., 2002 Evaluating and minimising social stress in the care of captive bottlenose dolphins (*Tursiops aduncus*). Zoo Biology 21:5–26.
Warburton K., Lazarus J., 1991 Tendency-distance models of social cohesion in animal groups. Journal of Theoretical Biology 150:473–488.
Whitham J. C., Wielebnowski N., 2013 New directions for zoo animal welfare science. Applied Animal Behaviour Science 147:247-260.

Received: 06 September 2023. Accepted: 25 November 2023. Published online: 15 December 2023.
Authors:
Kaori Tage, Graduate School of Fisheries Sciences, Hokkaido University 3-1-1 Minato, Hakodate, Hokkaido 041-8611, Japan, e-mail: kaori.t.fnawp07@gmail.com
Masatoshi Tsunokawa, Otaru Aquarium Co., Ltd. 3-303 Shukutsu, Otaru, Hokkaido 047-0047, Japan, e-mail: mtsuno@otaru-aq.jp
Hajime Ishikawa, Institute of Osaka Marine Research 703-15 Moriura, Taiji, Wakayama 619-5172, Japan, e-mail: ishikawa@dolphinresort.jp
Takashi Fritz Matsuishi, GCF, Faculty of Fisheries Sciences, Hokkaido University 3-1-1 Minato, Hakodate, Hokkaido 041-8611, Japan, e-mail: catm@fish.hokudai.ac.jp

How to cite this article:
Tage K., Tsunokawa M., Ishikawa H., Matsuishi T. F., 2023 A method to quantify social relationships between captive odontocetes based on distances between individuals during synchronous breathing. AACL Bioflux 16(6):3227-3239.